Accepted Manuscript

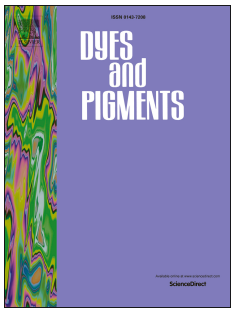

Alternating polymers based on alkoxy-phenyl substituted indacenodithiophene and fluorinated quinoxaline derivatives for photovoltaic cells

Weiping Wang, Baofeng Zhao, Haimei Wu, Shuo Liu, Hongli Liu, Zhaoqi Guo, Wei Wei, Chao Gao

PII: S0143-7208(17)30850-1

DOI: 10.1016/j.dyepig.2017.06.023

Reference: DYPI 6044

To appear in: *Dyes and Pigments*

Received Date: 17 April 2017

Revised Date: 23 May 2017

Accepted Date: 10 June 2017

Please cite this article as: Wang W, Zhao B, Wu H, Liu S, Liu H, Guo Z, Wei W, Gao C, Alternating polymers based on alkoxy-phenyl substituted indacenodithiophene and fluorinated quinoxaline derivatives for photovoltaic cells, *Dyes and Pigments* (2017), doi: 10.1016/j.dyepig.2017.06.023.

Alternating Polymers Based on Alkoxy-Phenyl Substituted Indacenodithiophene and Fluorinated Quinoxaline Derivatives for Photovoltaic Cells

Weiping Wang, [a,†] Baofeng Zhao, [a, †] Haimei Wu, [a] Shuo Liu, [b] Hongli Liu, [a] Zhaoqi Guo, [a] Wei Wei, [b] Chao Gao [a,*]

[a] State Key Laboratory of Fluorine & Nitrogen Chemicals, Xi'an Modern Chemistry Research Institute, Xi'an, Shaanxi, 710065, P. R. China.

[b] Nanjing University of Posts and Telecommunications, Nanjing 210003, P. R. China.

[†] These authors contributed equally to this work.

Abstract: To effectively modulate the molecular energy levels of indacenodithiophene (IDT)-based donor-acceptor (D-A) polymers, 4-hexyloxy-phenyl and 3-fluorine-4-hexyloxy-phenyl substituted IDT derivatives were designed and copolymerized with fluorinated quinoxaline derivatives (0F, 1F and 2F) to construct a series of novel alternating polymers. The effects of the side-chain modification in IDT units and the inclusion of fluorine atoms on quinoxaline units on the absorption performances, energy levels, hole transporting properties and photovoltaic performances of the resulting polymers were systemically studied. All polymers show high molecular weight, good solubility in common solvents, excellent thermal stabilities, finely tunable bandgaps and gradient adjusted energy levels. Above 5% power conversion efficiencies (PCEs) were achieved for all six polymers in conventional structural solar cells blending with [6,6]-phenyl-C71 butyric acid methyl ester ($PC_{71}BM$), in which the 3-fluorine-4-hexyloxy-

phenyl substituted IDT and quinoxaline based polymer (**FO-TQ**) showed a high PCE of 5.97% due to its high hole mobility and suitable energy level.

Keywords: Alternating polymers, Alkoxy-phenyl substituted indacenodithiophene, Fluorinated quinoxaline derivatives, Photovoltaic Cells.

1. Introduction

Polymer solar cells (PSCs) have attracted much attention in recent years due to their advantages of low-cost, lightweight, and flexibility. [1-3] Up till now, above 11% power conversion efficiency (PCE) in single active layer devices have been achieved in bulk heterojunction (BHJ), [4-9] in which the conjugated donor polymers have broad absorption spectra, high hole mobilities and low-lying highest occupied molecular orbital (HOMO) energy levels are the key driving force. Through combining electron-rich and electron-withdrawing units in one backbone, a variety of novel donor-acceptor (D-A) polymers possessing high performances have been developed. [10] Getting insight into the structures of the various D-A polymers, one excellent electron-rich donor unit is indacenodithiophene (IDT) for its planarity structure to provide enhanced electron delocalization and thus high charge-carrier mobility. [11] Many promising polymers had been designed and fabricated by the incorporation of IDT unit and multifarious electron-withdrawing moieties, [12-15] in which 4-hexyl-phenyl side-chains were included to the IDT unit to ensure the solubility of the resulting polymers in common solvents for the film fabrications.

It was demonstrated that the side-chains both in D and A segments could finely modulate the energy levels, bandgaps, charge transport properties and even the morphology and domain size of the polymers in the active layers. [16-22] By using 3-hexyl-phenyl instead of 4-hexyl-phenyl

as side chain, a relatively deep HOMO energy level and thus enhanced open circuit voltage (V_{oc}) and PCE (7.5%) had been accomplished for an indacenodithiophene-quinoxaline based polymer (PIDTTQ-m). [23] Very recently, using 5-hexyl-thienyl or 3-hexyl-phenyl groups as out-of-plane side-chains to replace the 4-hexyl-phenyl group, tunable energy levels and high performances were achieved for the side-chain modified small molecular non-fullerene acceptors (ITIC-Th and m-ITIC). [24,25] So the side-chains and their position on the phenyl groups of the IDT units are particularly important to construct promising donor or acceptor materials with desirable properties. Compare to alkyl groups, the alkoxy substituents in the donor segment possess relatively strong electron-donating ability, which are favourable to the absorptive properties of the polymers. [26,27]

As is well known, adjustment of molecular energy levels is one of the most important themes in the structural design of donor polymer because open-circuit voltages (V_{oc}) of PSCs are closely dependent on the gaps between the HOMO levels of the electron donors and the lowest unoccupied molecular orbital (LUMO) of the electron acceptor materials in their active layers. [28] Since the LUMO energy level of [6,6]-phenyl-C71 butyric acid methyl ester ($PC_{71}BM$) is fixed as -3.91eV, [29] deepening the electron-donor polymeric HOMO energy levels is an effective approach to achieve improved V_{oc} and photovoltaic properties for $PC_{71}BM$-based PSCs. There are two methods have been mainly used to modulate the molecular energy levels of conjugated polymers. First, introduction of strong electron-withdrawing groups (i.e. fluorine atom, [30] ketone, [31] sulfonyl group [32] and cyano group [33]) onto the A-units of D-A polymer and according to this method, improved V_{oc} and PCEs have been achieved in a variety of D-A polymers. Second, decreasing the electron-donor ability of the D-unit to therefore prepare so-called ‘weak-donor-strong-acceptor’ polymers is alternative way to obtain deep

HOMO energy levels. [34] In line with this method, fluorinated side chains pending on the D-units were prepared in several D-A polymers. [35,36] As expected, lowered HOMO energy levels and enhanced photovoltaic properties were accomplished.

On the basis of the above consideration, to systematically investigate alkoxy-phenyl-IDT-based D-A polymers and effectively modulate their energy levels, we herein synthesized six D-A polymers through the copolymerization of 4-hexyloxy-phenyl and 3-fluorine-4-hexyloxy-pheneyl substituted IDT derivatives with three quinoxaline derivatives (**Scheme 1**). The fluorinated quinoxaline derivatives (0F, 1F and 2F) are adopted as electron-withdrawing units due to their excellent electron-deficient N-heterocycle structure and facile synthesis process. [16, 37-39] The obtained polymers show excellent thermal stabilities and gradient adjusted HOMO energy levels. Moderate PCEs (>5%) are obtained for the polymers/$PC_{71}BM$-based conventional solar cells, with the best PCE value of 5.97% for the 3-fluorine-4-hexyloxy-phenyl substituted IDT and quinoxaline based polymer (FO-TQ).

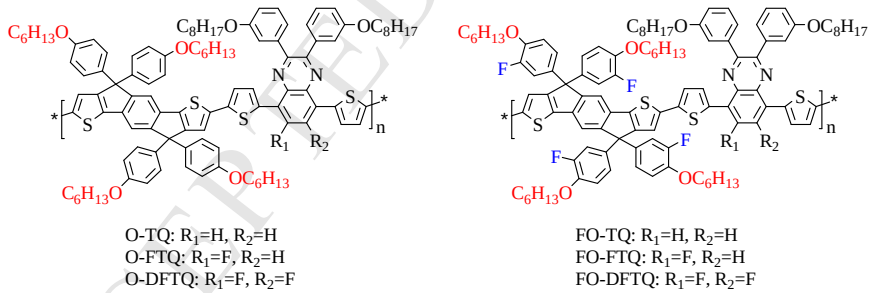

Scheme 1. Chemical structures of the polymers.

2. Experimental Section

2.1 Materials

All chemicals and solvents were purchased from Aldrich or Alfa & Aesar. Tetrahydrofuran (THF) is dried over sodium (Na) /benzophenone ketyl and freshly distilled prior to use. The synthetic routes of the monomers and polymers are shown in **Scheme 2**. The monomers 5,8-

bis(5-bromothiophen-2-yl)-2,3-bis(3-(octyloxy)phenyl)quinoxaline (**M3**), 5,8-Bis(5-bromothiophen-2-yl)-6-fluoro-2,3-bis(3-(octyloxy)phenyl) quinoxaline (**M4**) and 5,8-Bis(5-bromothiophen-2-yl)-5,6-di-fluoro-2,3-bis(3-(octyloxy)phenyl)quinoxaline (**M5**) were synthesized according to the literature. [37-39]

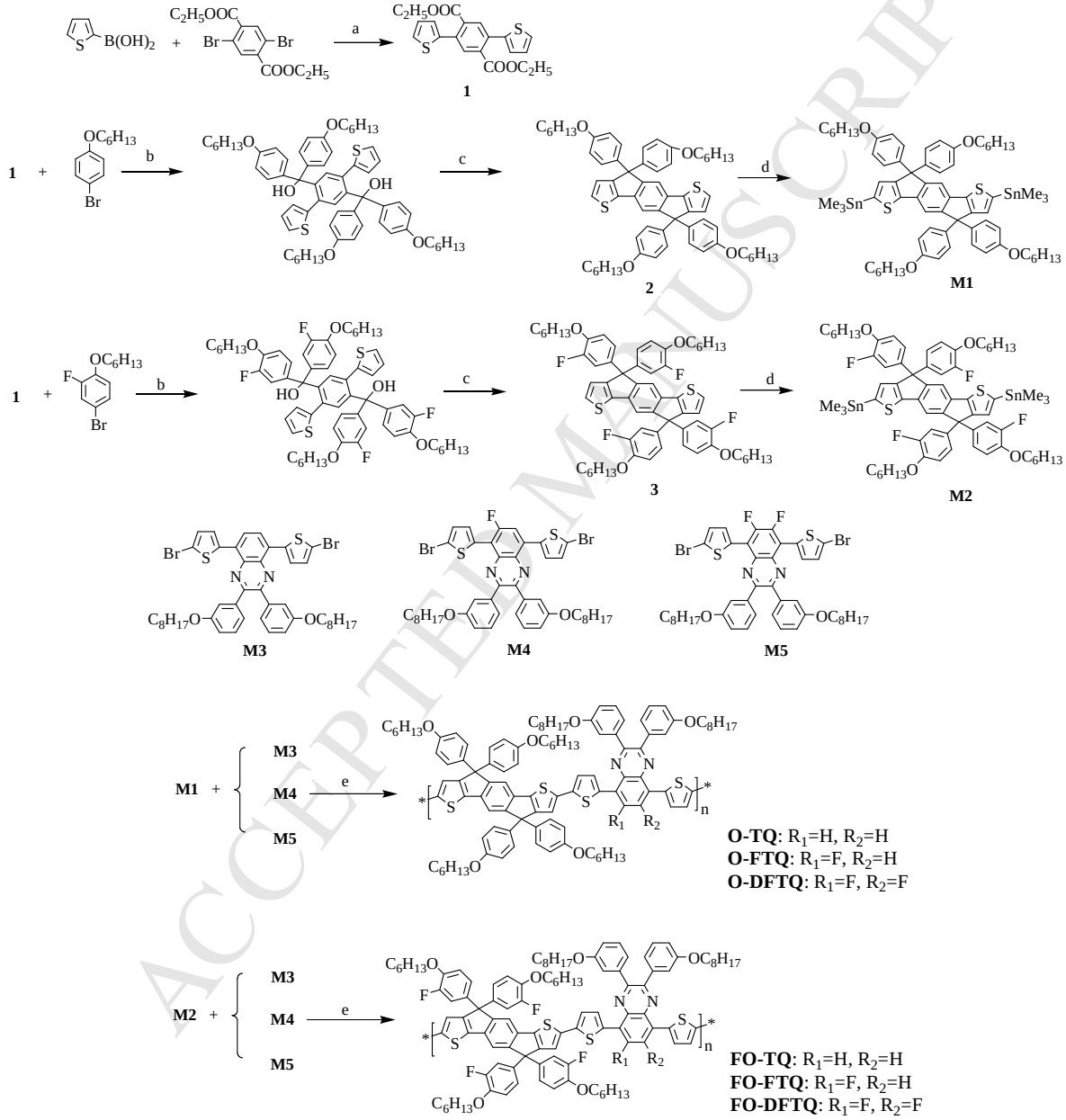

Scheme 2. The synthetic routes of the polymers. (a) THF, $Pd(AcO)_2/PPh_3$. (b,c) n-BuLi, -78 ^oC,then room temperature; CH_3COOH/H_2SO_4. (d) THF, n-BuLi, Me_3SnCl, -40 ^oC. (e) $Pd_2(dba)_3$, P(o-Tol)$_3$, toluene.

Diethyl-2,5-di(thiophen-2-yl)terephthalate (1).

To a solution of thiophen-2-ylboronic acid (3.20 g, 25 mmol) and diethyl 2,5-dibromo-terephthalate (3.80 g, 10 mmol) in THF (80 mL) was added saturated solution of sodium carbonate (15 ml), then ($Pd(AcO)_2$) (40 mg) and triphenylphopine (PPh_3) (80 mg) were added under nitrogen. After stirred at 70 ^oC overnight, the reaction was quenched with 100 mL water and extracted with ethyl acetate. Then, the combined organic solvent was washed with brine and dried over anhydrous magnesium sulfate ($MgSO_4$). After removing the solvent, the compound **1** was purified with column chromatography on silica-gel using mixture of ethyl acetate (EA) and hexane (1: 5 by volume) as a white solid (3.14 g, 81.3%). ^1H NMR (500 MHz, $CDCl_3$, ppm), δ 7.81 (s, 2H), 7.39 (dd, J = 5 Hz, J = 1 Hz, 2H), 7.08 (m, 4H), 4.21 (q, J = 5 Hz, 4H), 1.15 (t, J = 5 Hz, 6H).

4,4,9,9-tetrakis(4-hexyloxyphenyl)-s-indaceno[1,2-b:5,6-b']dithiophene (2)

To a solution of 4-hexyloxy-1-bromobenzene (6.4 g, 25 mmol in THF (30 mL) at -78 ^oC was added n-BuLi (10 mL, 2.5 M in hexane) under nitrogen, then the mixture was kept stirring at -78 ^oC for 1 h. After that a solution of compound 1 (1.93 g, 5 mmol) in THF (20 mL) was added slowly and then stirred overnight at room temperature. Water was added to quench the reaction and the mixture was extracted with dichloromethane. After the removal of solvent, the crude product was charged into 100 mL flask and acetic acid (50 mL) and concentrated sulfuric acid (1 mL) were added. Then the mixture was refluxed for 2 h. After pouring into water, the mixture was extracted with chloroform ($CHCl_3$) and washed with brine. The resulting crude compound was purified by silica gel to give a white solid **2** (2.95g, 61%). ^1H NMR (500 MHz, $CDCl_3$, ppm), δ 7.39 (s, 2H), 7.23 (m, 2H), 7.14 (d, J = 5 Hz, 8H), 6.96 (m, 2H), 6.76 (d, J = 5 Hz, 8H), 3.90 (t, J = 5 Hz, 8H), 1.74 (br, 8H), 1.42 (br, 8H), 1.31 (br, 16H), 0.88 (t, J = 5 Hz, 12H). ^{13}C NMR

(125 MHz, $CDCl_3$, ppm), δ 157.9, 156.1, 153.7, 141.0, 136.7, 134.9, 129.0, 127.4, 122.9, 117.2, 114.1, 67.9, 61.8, 31.5, 29.2, 25.7, 22.5, 14.0.

4,4,9,9-Tetrakis(3-fluoro-4-hexyloxyphenyl)-s-indaceno[1,2-b:5,6-b']dithiophene (3)

This compound was synthesized basing on 2-fluoro-4-bromo-1-(hexyloxy)benzene (8.25 g, 30 mmol) and compound 1 (2.28 g, 6 mmol) through the same routine as compound 2. Compound 3 was obtained as a white solid (3.8g, 62%). ^{1}H NMR (500 MHz, $CDCl_3$, ppm), δ 7.37 (s, 2H), 7.28 (d, 2H), 6.97 (br, 6H), 6.91 (dd, 4H), 6.82(m, 4H), 3.97 (t, J = 5 Hz, 8H), 1.78 (br, 8H), 1.33-1.30 (br, 24H), 0.89 (t, J = 5 Hz, 12H). ^{13}C NMR (125 MHz, $CDCl_3$, ppm), δ 155.1, 153.2, 151.3, 146.2, 141.2, 137.0, 135.0, 128.2, 123.4, 122.6, 117.2, 116.0, 114.4, 69.4, 61.5, 31.5, 29.1, 25.5, 22.5, 13.9.

4,4,9,9-Tetrakis(4-hexyloxyphenyl)-s-indaceno [1,2-b:5,6-b']dithiophene-2,7-diyl)bis(trimethylstannane) (M1)

Compound **2** (2.94 g, 3 mmol) and trimethylethyldiamine (0.45ml, 3mmol) was dissolved in 60 ml of anhydrous tetrahydrofuran (THF) and 10 ml of anhydrous hexane in a three-neck flask under the protection of argon. The solution was cooled to -40 ^{o}C and n-BuLi (2.5 M in hexane, 3.3ml) was added dropwise with stirring in 15 min. After that, the mixture was allowed to stir at ambient temperature for 30min. Then the reactant was cooled to -40 ^{o}C and trimethyltin chloride (2.7g, 9mmol) was added and stirred at -40 ^{o}C for 2h. Subsequently, the mixture was warmed to room temperature and poured into water. After extracted with ethyl acetate, the organic layer was dried over anhydrous magnesium sulfate ($MgSO_4$) and concentrated to afford the yellow crude product. After recrystallized twice from mixture of ethanol and hexane, monomer **M1** was finally obtained as a white crystal (2.91g, 75% yield). ^{1}H NMR (500 MHz, $CDCl_3$, ppm), δ 7.34 (s, 2H), 7.14 (d, 8H), 6.98 (s, 2H), 6.75(d, 8H), 3.89 (t, J = 5 Hz, 8H), 1.75 (br, 8H), 1.43 (br,

8H), 1.30 (br, 16H), 0.89 (t, J = 5 Hz, 12H), 0.33 (s, 18H). ^{13}C NMR (125 MHz, $CDCl_3$, ppm), 157.9, 157.8, 153.9, 147.1, 141.1, 137.1, 134.6, 130.4, 129.1, 117.5, 114.1, 67.9, 61.3, 31.6, 29.3, 25.7, 22.6, 14.0, -8.0.

4,4,9,9-Tetrakis(3-fluoro-4-hexyloxyphenyl)-s-indaceno[1,2-b:5,6-b'] dithiophene-2,7-diyl)bis(trimethylstannane) (M2)

Same process was adopt as **M1**, using compound **3** (3.12 g, 3 mmol) and trimethyltin chloride (2.7g, 9mmol) to obtain **M2** as a yellow crystals (2.55g, 72% yield). ^{1}H NMR (500 MHz, $CDCl_3$, ppm), δ 7.32 (s, 2H), 6.98 (br 6H), 6.91 (dd, 4H), 6.81 (t, 4H), 3.97 (t, J = 5 Hz, 8H), 1.78 (br, 8H), 1.33-1.30 (br, 24H), 0.89 (t, J = 5 Hz, 12H), 0.33 (s, 18H). ^{13}C NMR (125 MHz, $CDCl_3$, ppm), δ 156.8, 153.3, 151.3, 147.2, 146.0, 142.3, 137.4, 134.7, 129.9, 123.4, 117.5, 116.2, 114.3, 69.4, 61.1, 31.5, 29.2, 25.6, 22.6, 14.0, -8.0.

Synthesis of the polymers.

M1 (91 mg, 0.07mmol) and **M3** (60mg, 0.07mmol) were dissolved in a 50ml dry flask in degassed toluene (15ml), the mixture was flushed with argon for 30 min, tris(dibenzylideneacetone)dipalladium(0) ($Pd_2(dba)_3$) (2.0 mg) and tri(o-tolyl)phosphine ($P(o\text{-}Tol)_3$) (2.6 mg) were added, then flushed with argon again. Then the mixture was vigorously stirred at 95 ^oC for 24 h. After cooling down, the solution was poured into methanol. The polymer was collected by filtration and Soxhlet extracted in order with methanol, hexane, and then with chloroform. The chloroform solution was concentrated to a small volume, and the polymer was precipitated by pouring this solution into methanol. Finally, the polymer was collected by filtration, dried under vacuum at 50 ^oC overnight and afforded **O-TQ** as a dark solid (77 mg, 65%).^{1}H NMR (500 MHz, $CDCl_3$, ppm), δ 8.11 (s, 2H), δ 7.83 (s, 2H), 7.47-7.36(br, 4H), 7.30-7.22 (br, 16H), 7.15-6.97 (m,

2H), 6.83-6.82 (m, 8H), 3.95-3.92 (m, 8H), 3.83-3.75(m, 4H), 1.85-1.75 (br, 8H), 1.60-1.44 (br, 12H), 1.33-1.20(br, 36H), 0.89-0.79 (br, 18H). Anal. Calcd for $(C_{108}H_{120}N_2O_6S_4)_n$: C 77.66, H 7.24. Found: C 77.01, H 6.92.

The other five polymers were synthesized according to the same route as that of **O-TQ**.

For **O-FTQ**, dark solid (83 mg, yield 70%). ^{1}H NMR (500 MHz, $CDCl_3$, ppm), δ 7.99 (s, 2H), δ 7.83 (s, 1H) 7.39-7.35(br, 4H), 7.29-7.17 (br, 16H), 7.05-6.97 (m, 2H), 6.83-6.82 (m, 8H), 3.93 (m, 8H), 3.82-3.75(m, 4H), 1.85-1.75 (br, 8H), 1.58-1.44 (br, 12H), 1.33-1.20(br, 36H), 0.90-0.83 (br, 18H). Anal. Calcd for $(C_{108}H_{119}FN_2O_6S_4)_n$: C 76.83, H 6.97. Found: C 76.17, H 6.97.

For **O-DFTQ**, dark solid (87 mg, yield 73%). ^{1}H NMR (500 MHz, $CDCl_3$, ppm), δ 8.02 (s, 2H), 7.40-7.37(br, 4H), 7.28-7.18 (br, 16H), 6.99-6.98 (m, 2H), 6.84-6.82 (m, 8H), 3.95-3.92 (br, 8H), 3.78-3.75(br, 4H), 1.85-1.75 (br, 8H), 1.54-1.44 (br, 12H), 1.33-1.18(br, 36H), 0.90-0.80 (br, 18H). Anal. Calcd for $(C_{108}H_{118}F_2N_2O_6S_4)_n$: C 76.02 H 6.97. Found: C 75.67, H 7.03.

For **FO-TQ,** dark solid (81 mg, 66%). ^{1}H NMR (500 MHz, $CDCl_3$, ppm), δ 8.04 (s, 2H), 7.74 (s, 2H), 7.31-7.12(br, 10H), 6.99-6.88 (m, 12H), 6.81-6.78 (br, 4H), 3.95-3.92 (m, 8H), 3.74 (m, 4H), 1.74-1.71 (br, 8H), 1.52-1.38 (br, 12H), 1.25-1.11(br, 36H), 0.82-0.71 (br, 18H). Anal. Calcd for $(C_{108}H_{116}F_4N_2O_6S_4)_n$: C 74.45, H 6.71. Found: C 74.17, H 6.66.

For **FO-FTQ**, dark solid (76 mg, 62%). ^{1}H NMR (500 MHz, $CDCl_3$, ppm), δ 8.01 (s, 2H), 7.84 (s, 1H), 7.41-7.28 (br, 10H), 7.15 (m, 2H), 7.06-6.86(br, 14H), 4.03-4.00 (m, 8H), 3.81-3.79 (m, 4H), 1.82-1.79 (br, 8H), 1.59-1.46 (br, 12H), 1.33-1.17(br, 36H), 0.90-

0.82 (br, 18H). Anal. Calcd for $(C_{108}H_{115}F_5N_2O_6S_4)_n$: C 73.69, H 6.58. Found: C 73.70, H 6.67.

For **FO-DFTQ**, dark solid (88 mg, 71%). ^{1}H NMR (500 MHz, $CDCl_3$, ppm), δ 8.04 (s, 2H), 7.40-7.16 (br, 10H), 7.16 (m, 2H), 7.06-6.86 (br, 14H), 4.01 (m, 8H), 3.78 (m, 4H), 1.82-1.79 (br, 8H), 1.54-1.46 (br, 12H), 1.33-1.17(br, 36H), 0.90-0.82 (br, 18H). Anal. Calcd for $(C_{108}H_{114}F_6N_2O_6S_4)_n$: C 72.94, H 6.46, Found: C 72.19, H 6.44.

2.2 Measurements

All the compounds were characterized by nuclear magnetic resonance spectra (NMR) recorded (Bruker AV 500 spectrometer) in chloroform-d at room temperature using tetramethylsilane (TMS) as an internal reference. The chemical shifts were accounted in ppm related to the singlet of $CDCl_3$ at 7.26 ppm and 77 ppm for ^{1}H and ^{13}C NMR, respectively. Molecular weights and distributions of polymers were estimated by gel permeation chromatography (GPC) method at 150 ^{o}C, 1,2,4-trichlorobenzene as eluent and polystyrene as standard. Thermogravimetric analysis (TGA) of the polymers was investigated on a Universal V2.6D TA instruments with a thermal rate of 10°C/min at N_2 atmosphere. The absorption spectra were determined by a PerkinElmer Lambda 750 UV/Vis/NIR spectrometer. Thermogravimetric analysis (TGA) of the polymers was investigated on a Universal V2.6D TA instruments. The electrochemical cyclic voltammetry was conducted on a CHI 660D Electrochemical Workstation with glassy carbon, Pt wire, and Ag/Ag^+ electrode as working electrode, counter electrode, and reference electrode respectively in a 0.1mol/L tetrabutylammonium hexafluorophosphate (Bu_4NPF_6) acetonitrile solution. Polymer thin films were formed by drop-casting chloroform solution (analytical reagent, 1mg/mL) onto the working electrode, and then dried in the air. Atomic force microscopy (AFM) images were collected in air under ambient conditions using the MultiMode scanning

probe microscope (AFM, Veeco MultiMode V). Thickness of the active layer was measured on a Bruker Dektak-XT surface profiler. Tansmission electron microscopy (TEM) was performed on a JEM-2100 (200 kV). Without the electrode deposition, the active layer was placed onto a copper grid after dissolving the PEDOT:PSS in water and then dried at room temperature.

2.3 Fabrication and characterization of PSCs

The device structure was ITO/poly(3,4-ethylenedioxythiophene):poly(styrene sulfonic acid) (PEDOT:PSS)/polymer:$PC_{71}BM$/poly[(9,9-dioctyl-2,7-fluorene)-*alt*-(9,9-bis(3-N,N-dimethylamino)propyl)-2,7-fluorene] (PFN)[31] /Al, a 40-nm-thick PEDOT:PSS anode buffer layer was spin-cast on the ITO substrate, then dried in a vacuum oven at 140 ^{o}C overnight. The polymer:$PC_{71}BM$ active layer was spin-coated through their 1,2-dichlorobenzene solution with various weight ratios in a nitrogen-filled glovebox (< 1ppm O_2 and H_2O). A 5 nm PFN layer was then spin-coated from methanol solution in presence of a trace amount of acetic acid onto the active layer. Subsequently, the films were transferred into a vacuum evaporator and 100 nm of Al were deposited as cathode under the vacuum of $<10^{-5}$ torr. The effective area of a device was 0.16 cm^2 which was determined by the shadow mask used during deposition of Al cathode. PCE values were determined from current density (*J*)-voltage *(V)* curve measurements (using a Keithley 2400 source meter) under 1 sun, AM 1.5G spectrum from a solar simulator (Newport model 94021A, 100 mW cm^{-2}). A monocrystal silicon cell (VLSI Standards Inc.) calibrated by the National renewable Energy laboratory (NREL) was used as a reference. The external quantum efficiency (EQE) of the devices was measured using a Hypermonolight System (QTEST 1000 AD, Crowntech Inc.).

2.4 Hole mobility measurement

The device structure of space charge limited current (SCLC) studies is ITO/PEDOT:PSS/polymer:$PC_{71}BM$/MoO_3(10nm)/Al with the effective area of 0.16 cm^2. The mobility was determined by fitting the dark current to the model of a single carrier SCLC, which is described by the equation: $J= (9/8)\varepsilon_0\varepsilon_r\mu((V^2)/(d^3))$, where J is the current, μ is the zero-field mobility, ε_0 is the permittivity of free space, ε_r is the dielectric constant of the polymer, d is the thickness of the active layer, and V is the effective voltage. The effective voltage can be obtained by subtracting the built-in voltage (V_{bi}) and the voltage drop (V_s) from the substrate's series resistance from the applied voltage (V_{appl}), $V=V_{appl}-V_{bi}-V_s$. The hole-mobility can be calculated from the slope of the $J^{1/2} \sim V$ curves.

3. Results and discussion

3.1 Materials design and synthesis

The synthetic routes of the six polymers are shown in **Scheme 2**. In our synthetic design, the 4-hexyloxy-phenyl and 3-fluorine-4-hexyloxy-phenyl substituted IDT units and fluorinated quinoxaline derivatives (0F, 1F and 2F) were taken as the D-units and A-units, respectively. All polymers were prepared via the typical Stille-coupling reaction with moderate yield between organotin monomers of IDT derivatives (**M1** and **M2**) and bromothiophene-flanked fluorinated quinoxaline derivatives (**M3**, **M4** and **M5**), using toluene as solvent, tris(dibenzylideneacetone) dipalladium ($Pd_2(dba)_3$) and tri(otolyl)phosphine ($P(o\text{-}tol)_3$) as catalyst. All the intermediates, monomers and the polymers were fully characterized by ^{1}H-NMR, ^{13}C-NMR, and elemental analysis (**Figure S1-S14**, ESI). The gel permeation chromatography (GPC) measured molecular weights and polydispersity index (PDI) of the six polymers are displayed in **Table 1**. All polymers exhibit high molecular weight (M_w) above 80 kDa. In contrast to the 3-fluorine-4-hexyloxyphenyl substituted polymers (**FO-TQ**, **FO-FTQ**, **FO-DFTQ**), the polymers (**O-TQ**, **O-**

FTQ and **O-DFTQ**) with 4-hexylxoy-phenyl side-chain display higher Mw, especially for the 4-hexyloxy-phenyl IDT and mono-fluorinated quinoxaline based polymer (**O-FTQ**) owns the highest Mw over 400 kDa, with a relatively narrow PDI of 1.65. All polymers show good solubility in chloroform, o-dichlorobenzene (oDCB) and other common solvents, which are conducive to the film fabrication.

3.2 Properties of the polymers

The thermal properties of the polymers were investigated by thermogravimetric analysis (TGA, **Figure S15**, ESI). All polymers have decomposition temperature (defined as the 5% weight-loss temperature, T_d) over 410 ^oC and the polymer **O-TQ** shows the highest T_d (452^oC) under nitrogen as determined by thermogravimetric analysis (TGA), indicating their excellent thermal stabilities.

The optical absorption properties of the polymers were investigated by ultraviolet-visible (UV-vis) absorption spectroscopy both in chloroform solutions (**Figure S16**, ESI) and in thin films (**Figure 1**). The detailed data obtained from the absorption spectra are summarized in **Table 1**. As shown in **Figure S16** and **Figure 1**, two main absorption bands are observed for the polymers both in chloroform solutions and in solid state films. The high-energy region absorption band in a range of 350-470 nm is ascribed to the π-π* transitions, and a low-energy region (470-700 nm) absorption band corresponding to the intramolecular charge transfer (ICT) between the IDT (D) and quinoxaline (A) unit. Unlike other D-A polymers with strong red-shifts absorption in the solid states, only slight red-shifts are investigated for all polymer films compare to the chloroform solutions, which indicate the polymers remain largely disordered in the solid state and are coincided with previously reported IDT-based polymers. [23] The absorption edges (λ_{edge})

of the films are located at 674 nm (**O-TQ**), 679 nm (**O-FTQ**), 675nm (**O-DFTQ**), 671 nm (**FO-TQ**), 667 nm (**FO-FTQ**) and 661nm (**FO-DFTQ**), respectively, corresponding to medium optical bandgaps ranged from 1.83 eV to 1.87 eV (**Table 1**). Relative to the 4-hexyloxy-phenyl substituted polymers (**O-TQ**, **O-FTQ** and **O-DFTQ**) possessing similar bandgaps of 1.83-1.84 eV, the 3-fluoro-4-hexyloxy-phenyl substituted polymers exhibit wide optical bandgaps (1.85eV for **FO-TQ**, 1.86 eV for **FO-FTQ** and 1.87 eV for **FO-DFTQ**), which are attributed to the inclusion of the electron-withdrawing fluorine atom on the IDT unit. Furthermore, it is worth noting that when 1F is introducing to the quinoxaline unit, slightly bigger or smaller optical bandgaps are simultaneously observed, which mainly because of the random location of the fluorine atom. [40] Relative to the 0F and 1F substituted quinoxaline-based polymers, the 2F substituted polymers show the largest bandgaps (1.84 eV for **O-DFTQ** and 1.87eV for **FO-DFTQ**), agreeing well with other 2F substituted polymers. [41]

In order to investigate the frontier energy levels of the polymers, cyclic voltammetry (CV) was employed to measure the oxidation and reduction potentials of the polymers films (**Figure S17**, ESI). For calibration, the redox potential of ferrocene/ferrocenium (Fc/Fc^+) was measured under the same conditions, and it was located at 0.09 V to the Ag/Ag^+ electrode under our measurement. It is assumed that the redox potential of Fc/Fc^+ has an absolute energy level of -4.80 eV to vacuum. [42] Then the HOMO energy levels (E_{HOMO}) of the polymers were determined from the onset oxidation potentials (E_{ox}) according to the following equations: $E_{HOMO}=-e(E_{ox} + 4.71)$ (eV), where the unit of potential is V vs Ag/Ag^+. [43] Subsequently, the lowest unoccupied molecular orbital (LUMO) energy levels (E_{LUMO}) can be calculated from the E_{HOMO} data and optical bandgaps of the polymers. According to the E_{ox} data, the calculated E_{HOMO}/E_{LUMO} values of the

polymers were -5.20/-3.36 eV (**O-TQ**), -5.21/-3.38 eV (**O-FTQ**), -5.26/-3.42 eV (**O-DFTQ**), -5.23/-3.38 eV (**FO-TQ**), -5.26/-3.40 eV (**FO-FTQ**) and -5.28/-3.41 eV for **FO-DFTQ**, respectively. Obviously, deeper HOMO energy levels for the 3-fluorine-4-hexyloxy-phenyl-based polymers (**FO-TQ**, **FO-FTQ** and **FO-DFTQ**) are observed in comparison to the 4-hexyloxy-phenyl-substituted polymers (**O-TQ**, **O-FTQ** and **O-DFTQ**), which can be attributed to the fluorine substituted on the IDT unit. Furthermore, the mono-fluorinated and di- fluorinated quinoxaline based copolymers display reduced HOMO levels relative to the non-fluorinated materials, which mainly due to the electron-withdrawing effect of the fluorine atoms on the A-unit. The 3-fluorine-4-hexyloxy-phenyl modified IDT and di-fluorinated quinoxaline based polymer **FO-DFTQ** displays the deepest HOMO energy level of -5.28 eV for the synergistic effect of the six fluorine atom in one repeating unit. To make a clear comparison, the gradient varied polymeric energy levels diagrams as well as the molecular energy levels of other used materials in this study are summarized in **Figure 2b**. Obviously, the LUMO energy levels of the polymers are significantly higher than that of $PC_{71}BM$ (-3.90 eV in our measurement), which facilitate electron transferring from the polymers to the $PC_{71}BM$ at the photoactive layer of PSCs.

To explore the electronic properties of the polymers, molecular simulations were also performed on two repeated donor-acceptor unit with all side chains reserved using the Density Functional Theory (DFT) at B3LYP/6-31G(d) level. [44] As shown in **Table S1**, the localization of HOMOs distributed along the polymer backbone while the LUMOs of both polymers are somewhat more localized on the quinoxaline units, indicating the significant charge-transfer character between IDT and quinoxaline segment, which are consistent with the observed strong low-energy absorption band in **Figure 1**. From the simulation data, the 3-fluoro-4-hexyloxy-

phenyl substituted polymers exhibit deeper HOMO energy levels, agreeing well with the CV measured data. The calculated energy levels of the polymers are also listed in **Table 1.**

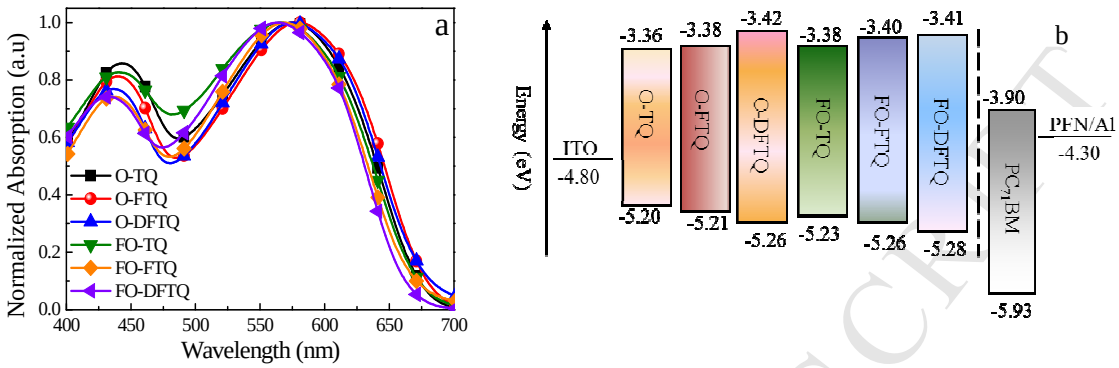

Figure 1. (a) Normalized absorption of the polymer films. (b) Schematic illustration of relative positions of HOMO/LUMO energy levels of the six polymers and other materials used in the PSCs.

Table 1. Optical, electrochemical and thermal properties of the polymers

Polymer	M_n	M_w	PDI	T_d [°C]	λ_{edge} [nm]	E_g^{opt} a) [eV]	HOMO b) [eV]	LUMO b) [eV]	E_{ox} c) [V]	HOMO c) [eV]	LUMO d) [eV]
O-TQ	71130	144030	2.02	452	674	1.84	-4.37	-2.24	0.49	-5.20	-3.36
O-FTQ	247921	409209	1.65	411	679	1.83	-4.39	-2.32	0.50	-5.21	-3.38
O-DFTQ	215204	380797	1.77	434	675	1.84	-4.43	-2.34	0.55	-5.26	-3.42
FO-TQ	45380	89028	1.96	444	671	1.85	-4.46	-2.30	0.52	-5.23	-3.38
FO-FTQ	88532	184869	2.09	434	667	1.86	-4.48	-2.38	0.55	-5.26	-3.40
FO-DFTQ	91357	241914	2.65	436	662	1.87	-4.52	-2.40	0.57	-5.28	-3.41

a) estimated from the onset of electronic absorption of the polymer films (E_g^{opt} =1240/λ_{edge}(nm)). b) calculated results from the DFT at B3LYP/6-31G(d) level. c) cyclic voltammetry results. d) calculated from the tested HOMO energy levels and the E_g^{opt}.

3.3 Characteristics and Optimization of Photovoltaic Devices

To investigate the photovoltaic properties of the obtained polymers, PSCs with a conventional device structure of ITO/PEDOT:PSS/polymer:$PC_{71}BM$/PFN/Al were fabricated. The photoactive layer were spin-coated on top of pre-fabricated PEDOT:PSS layer from their 1,2-dichlorobenzene solution. Then the blend film was pre-thermal annealed at 70 °C for 10 min and followed by a THF solvent vapor annealing (SVA) of 35 sec to obtain the optimized morphology of the active layer. After that, a 5 nm

water/alcohol soluble PFN [45] as the electron-collecting layer was spin-coated atop photoactive layer before deposition of cathode. SVA has been considered as an effective post-treatment method for organic photovoltaic cells due to its universality to optimize the active layer morphology and improve the charge transport properties. [46,47] THF SVA 35 sec was chosen as the post-treated condition for its effectiveness in improving the performances of quinoxaline-based polymers, which were according to the literatures and our previous results.[16,39,48] The device performances of both polymers are critically dependent on the polymer:$PC_{71}BM$ weight ratios in their active layer. Optimal weight ratios for the polymers and $PC_{71}BM$ blends are almost the same as 1:3, except for the polymer **O-FTQ** (1:2). (**Figure S18** and **Table S2**). The current density versus voltage (*J-V*) characteristics and the external quantum efficiency (EQE) curves of the corresponding optimized PSCs under AM 1.5 G at 100 mW cm^{-2} illumination are presented in **Figure 2**. Photovoltaic parameters deduced from the corresponding *J-V* curves are summarized in **Table 2**. Both six polymers showed moderate PCE values (>5%) with slightly differences under their optimal device condition. Compare to the 3-fluorine-4-hexyloxy-phenyl modified polymers, the 4-hexyloxy-phenyl-based polymers exhibit slightly higher short-current density (J_{sc}) and **O-FTQ** possesses the highest J_{sc} of 11.07 mA cm^{-2}, which is ascribed to its small bandgap. As we known, higher molecular weight (Mw) of the amorphous conjugated polymer like PTB7 leads to enhanced J_{sc} in PSCs.[49] Therefore, the slightly improved J_{sc} of **O-FTQ** and **O-DFTQ**-based devices can also be ascribed to their higher Mw. As for the 3-fluoro-4-hexyloxy-phenyl substituted polymers, higher open-circuit voltage (V_{oc}) values are achieved with the biggest V_{oc} of 0.97 V for **FO-DFTQ**-based device as anticipation, due to their deep

HOMO energy levels as illuminated above. It have been reported that the inclusion of fluorine in the conjugated polymer can effectively increase the dielectric constant to reduce the energy loss between polymers and PCBM. [38,41a] The higher V_{oc} values of the fluorinated polymers are also be the results of the increased dielectric constants.

As shown in **Figure 2a** and **2b**, the devices of these six polymers processed under each optimal conditions show slightly different EQE plots. The maximum responding wavelength is 400 nm corresponding the EQE peak value of 56.3% for **O-TQ**, 423 nm for **O-FTQ** (61.4%), 399 nm for **O-DFTQ** (59.1%), 455 nm for **FO-TQ** (60.8%), 451 nm for **FO-FTQ** (60.7%) and 451 nm for **FO-DFTQ** (57.9%), respectively. For the three 3-fluoro-4-hexyloxy-phenyl substituted polymers, relatively low EQE responses are observed which are agreed with their small J_{sc}. Although moderate V_{oc} and J_{sc} are observed, the **FO-TQ** and **FO-FTQ**-based device exhibit high FF of 65% and 66%, leading to enhanced PCE of 5.97% and 5.92%. Clearly, the slightly better photovoltaic performances in the **FO-TQ** and **FO-FTQ**-based devices mainly attributed to the high FF, indicating their better charge transport behaviour as discussed below.

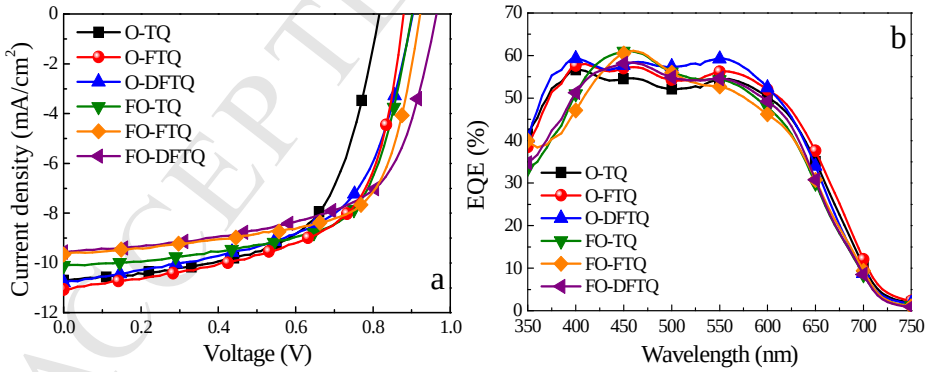

Figure 2. (a) The *J*-V curves of PSCs based on polymer:$PC_{71}BM$ under their optimal donor:acceptor ratios; (b) the corresponding EQE curves.

Table 2. Photovoltaic performances of the six copolymers measured under illumination of AM 1.5 G condition, 100 mW cm^{-2}

Polymer	Polymer:$PC_{71}BM$[w/w]	V_{oc} [V]	J_{sc} [mA cm^{-2}]	FF	PCE[a] [%]	μ_{hole} [cm^{2}V^{-1}s^{-1}]

O-TQ	1:3	0.83	10.70	0.61	5.37 (5.12)	1.48×10^{-4}
O-FTQ	1:2	0.88	11.07	0.60	5.84 (5.65)	1.04×10^{-4}
O-DFTQ	1:3	0.91	10.79	0.57	5.59 (5.32)	3.35×10^{-5}
FO-TQ	1:3	0.91	10.10	0.65	5.97 (5.83)	5.37×10^{-4}
FO-FTQ	1:3	0.93	9.65	0.66	5.92 (5.71)	1.12×10^{-3}
FO-DFTQ	1:3	0.97	9.56	0.61	5.66 (5.42)	3.46×10^{-4}

[a] The average value from 8 individual devices is given in parentheses

3.4 Charge Transport Properties and morphology of the polymers

To illuminate the morphologies of the six polymers based devices, atomic force microscopy (AFM) study was carried out to investigate the phase-separated morphologies of the polymers:$PC_{71}BM$ blends corresponding to the best performance, which were shown in **Figure 3**. All six blends exhibit interpenetrating feature with bicontinuous network between polymer and $PC_{71}BM$ and show quite smooth surface with small root-mean-square roughness (RMS) value of less than 0.6 nm, indicating the good miscibility of the polymer with $PC_{71}BM$. To explore the morphology throughout the active layer, TEM was employed to investigate the real-space structures of the polymer/$PC_{71}BM$ blend films, which can be seen in **Figure 4.** Blend films of **O-TQ**, **O-FTQ**, **FO-FTQ** and **FO-DFTQ** form fine phase separations (1–10 nm). For the **O-DFTQ** and **FO-TQ** blend film, obvious $PC_{71}BM$ aggregates are founed, which are consistent with the observed higher RMS values in AFM. Polymer aggregation cooresponding to the bright dots in **Figure 4** are found for the **O-FTQ**, **FO-TQ** and **FO-FTQ**-based blends, indicating their good hole transporting abilities.

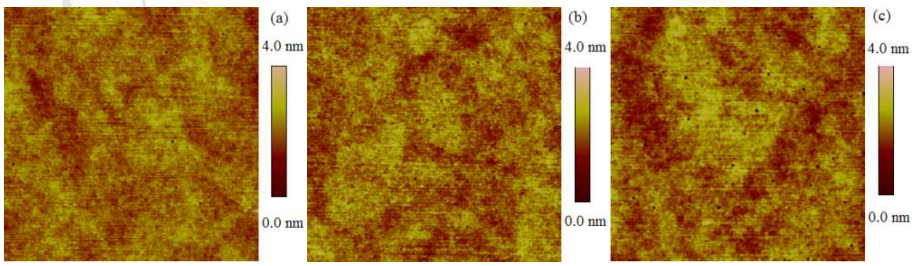

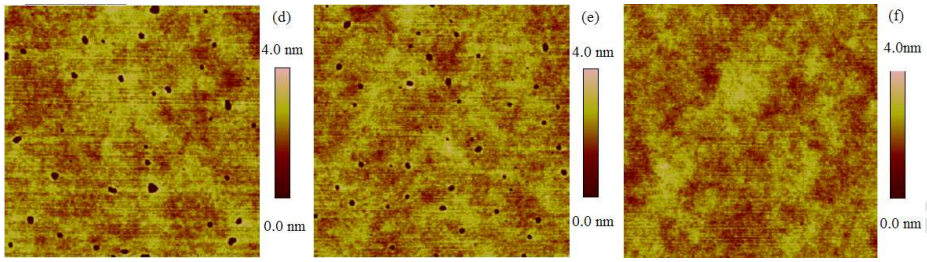

Figure 3. AFM topography images (4 μm ×4 μm) of ITO/PEDOT:PSS/Polymer:$PC_{71}BM$.(a): **O-TQ**:$PC_{71}BM$ (1:3) blend film (RMS: 0.35 nm); (b) **O-FTQ**:$PC_{71}BM$ (1:3) blend film (RMS: 0.37 nm); (c) **O-DFTQ**:$PC_{71}BM$ (1:3) blend film (RMS: 0.40 nm); (d) **FO-TQ**:$PC_{71}BM$ (1:3) blend film (RMS: 0.61 nm); (e) **FO-FTQ:**$PC_{71}BM$ (1:3) blend film (RMS: 0.56 nm) and (f) **FO-DFTQ**:$PC_{71}BM$ (1:3) blend film (RMS: 0.37 nm).

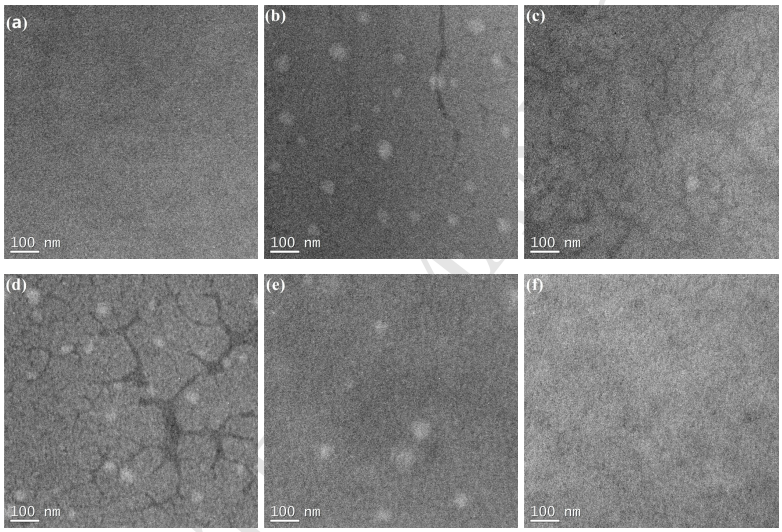

Figure 4. TEM bright field images of the optimized polymer:PC71BM blend films (a) **O-TQ**; (b) **O-FTQ**; (c) **O-DFTQ**; (d) **FO-TQ**:$PC_{71}BM$; (e) **FO-FTQ** and (f) **FO-DFTQ** blend film.

The hole mobility (μ_h) is crucial to achieve balance charge transport across the device, we used space-charge limited current (SCLC) method to measure the hole mobility in a device structure of ITO/PEDOT:PSS/polymer:$PC_{71}BM/MoO_3$/Al, and the results are plotted in **Figure S19** (ESI) and summarized in **Table 2**. The obtained hole mobility is 1.48×10^{-4} $cm^2V^{-1}s^{-1}$ for **O-TQ**, 1.04×10^{-4} $cm^2V^{-1}s^{-1}$ for **O-FTQ**, 3.35×10^{-5} $cm^2V^{-1}s^{-1}$ for **O-DFTQ**, 5.37×10^{-4} $cm^2V^{-1}s^{-1}$ for **FO-TQ**, 1.12×10^{-3} $cm^2V^{-1}s^{-1}$ for **FO-FTQ** and 3.46×10^{-4} cm^2 V^{-1} s^{-1} for **FO-DFTQ**, respectively. The 4-hexyloxy-phenyl substituted polymers exhibit relatively low hole mobility

which result in their small FF. However, improved hole mobilities are observed for the 3-fluorine-4-hexyloxy-phenyl substituted polymers, which are contributed to the higher FF values and are accorded with the reported hole mobility values of fluorinated polymers in the literature.[50] Despite the different V_{oc} and J_{sc}, **FO-TQ** and **FO-FTQ** possess high hole mobilities of 5.37×10^{-4} and 1.12×10^{-3} $cm^2 V^{-1} s^{-1}$, which give rise to the similar high FF (65% vs. 66%) and PCE value (5.97% vs. 5.92%).

4. Conclusion

In summary, six D-A polymers based on 4-hexyloxy-phenyl and 3-fluorine-4-hexyloxy-phenyl substituted IDT and fluorinated quinoxaline derivatives (0F, 1F and 2F) with excellent thermal stability were synthesized and characterized. The inclusion of fluorine atoms both in donor unit and in acceptor unit can effectively modulate the energy levels and absorptive behaviors of the polymers. Benefit from their high hole mobility and suitable molecular energy level, the 3-fluorine-4-hexyloxy-phenyl substituted IDT and quinoxaline based polymer (**FO-TQ**) exhibit an open-circuit voltage (V_{oc}) of 0.91V, a short-circuit current (J_{sc}) of 10.10 mA/cm^2, and an improved fill factor (FF) of 65 %, leading to a high power conversion efficiency (PCE) of 5.97%. Consideration the obtained gradient adjusted energy levels of the polymers through incorporation with side-chain modification and fluorinated both in the D and A-unit, we believe that these results can promote the design and synthesis of novel D-A polymers with deep HOMO energy levels.

Acknowledgements

We would like to thank the financial support of the National Natural Science Foundation of China (No. 21504067).

Appendix A. Supplementary data

Supplementary data related to this article can be found at http://dx.doi.org/10.1016/j.dyepig.

REFERENCES

[1] (a) Li Y. Molecular Design of Photovoltaic Materials for Polymer Solar Cells: Toward Suitable Electronic Energy Levels and Broad Absorption. Accounts of Chemical Research. 2012;45(5): 723-733. (b) Lu L, Zheng T, Wu Q, Schneider AM, Zhao D, Yu L. Recent Advances in Bulk Heterojunction Polymer Solar Cells. Chemical Reviews. 2015;115(23):12666–12731.(c) Lu L, Chen W, Xu T, Yu L. High-performance ternary blend polymer solar cells involving both energy transfer and hole relay processes. Nature Communications. 2015;6:7327

[2] Yu G, Gao J, Hummelen JC, Wudl F, Heeger AJ. Polymer photovoltaic cells -enhanced efficiencies via a network of internal donor-acceptor heterojunctions : Enhanced Efficiencies via a Network of Internal Donor-Acceptor Heterojunctions. Science. 1995;270(5243):1789-91.

[3] Henson ZB. Müllen K, Bazan GC. Design strategies for organic semiconductors beyond the molecular formula. Nature Chemistry. 2012;4(9): 699–704.

[4] Liao SH, Jhuo HJ, Yeh PN,Cheng YS, Li YL, Lee YH, Sharma S, Chen SA. Single Junction Inverted Polymer Solar Cell Reaching Power Conversion Efficiency 10.31% by Employing Dual-Doped Zinc Oxide Nano-Film as Cathode Interlayer. Scientific Reports. 2014;4: 6813.

[5] Zheng Z, Zhang S, Zhang J, Qin Y, Li W, Yu R, Wei Z, Hou J. Over 11% Efficiency in Tandem Polymer Solar Cells Featured by a Low-Band-Gap Polymer with Fine-Tuned Properties. Advanced Materials. 2016;28(25):5133-38.

[6] Liu Y, Zhao J, Li Z, Mu C, Ma W, Hu H, Jiang K, Lin H, Ade H, Yan H. Aggregation and morphology control enables multiple cases of high-efficiency polymer solar cells. Nature Communications. 2014:5: 5293.

[7] Zhao J, Li Y, Yang G, Jiang K, Lin H, Ade H, Ma W, Yan H. Efficient organic solar cells processed from hydrocarbon solvents. Nature Energy. 2016;1: 15027.

[8] He Z, Xiao B, Liu F, Wu H, Yang Y, Xiao S, Wang C, Russell TP, Cao Y, Single-junction polymer solar cells with high efficiency and photovoltage. Nature Photonics, 2015;9:174-179.

[9] Ouyang X, Peng R, Ai L, Zhang X, Ge Z. Efficient polymer solar cells employing a non-conjugated small-molecule electrolyte. Nature Photonics, 2015;9:520-524.

[10] (a) Wang E, Wang L, Lan L, Luo C, Zhuang W, Peng J, Cao Y. High-performance polymer heterojunction solar cells of a polysilafluorene derivative. Applied Physics Letters. 2008;92:033307. (b) Park SH, Roy A, Beaupre S, Cho S, Coates N, Moon JS, Moses D, Leclerc M, Lee K, Heeger AJ. Bulk heterojunction solar cells with internal quantum efficiency approaching 100%. Nature Photonics. 2009;3:297-302. (c) Qin R, Li W, Li C, Du C, Veit C, Schleiermacher HF, Andersson M, Bo Z, Liu Z, Inganäs O, Wuerfel U, Zhang F. A Planar Copolymer for High Efficiency Polymer Solar Cells. Journal of the American Chemical Society. 2009;131(41):14612-13. (d) Liang Y, Xu Z, Xia J, Tsai ST, Wu Y, Li G, Ray C, Yu L. For the Bright Future-Bulk Heterojunction Polymer Solar Cells with Power Conversion Efficiency of 7.4%. Advanced Materials. 2010;22(20): E135-E138. (e) Zou Y, Najari A, Berrouard P, Beaupré S, Aïch BR, Tao Y, Leclerc M. A Thieno[3,4-c]pyrrole-4,6-dione-Based Copolymer for Efficient Solar Cells. Journal of the American Chemical Society. 2010; 132 (15):5330–31. (f) Amb CM, Chen S, Graham KR, Subbiah J, Small CE, So F, Reynolds JR. Dithienogermole As a Fused Electron Donor in Bulk Heterojunction Solar Cells. Journal of the American Chemical Society. 2011; 133 (26):10062–65. (g) Wang E, Ma Z, Zhang Z, Vandewal K, Henriksson P, Inganas O, Zhang F, Andersson MR. An Easily Accessible Isoindigo-Based Polymer for High-

Performance Polymer Solar Cells. Journal of the American Chemical Society. 2011;133 (36):14244-47.
[11] Xu YX, Chueh CC, Yip HL, Ding FZ, Li YX, Li CZ, Li X, Chen WC, Jen AK. Improved Charge Transport and Absorption Coefficient in Indacenodithieno[3,2-b]thiophene-based Ladder-Type Polymer Leading to Highly Efficient Polymer Solar Cells. Advanced Materials. 2012;24(47):6356-61.
[12] Chen S, Lee KC, Zhang ZG, Kim DS, Li Y, Yang C. An Indacenodithiophene-Quinoxaline Polymer Prepared by Direct Arylation Polymerization for Organic Photovoltaics. Macromolecules. 2016;49(2): 527-536.
[13] Zhang W, Han Y, Zhu X, Fei Z, Feng Y, Treat ND, Faber H, Stingelin N, McCulloch I, Anthopoulos TD, Heeney M. A Novel Alkylated Indacenodithieno[3,2-b]thiophene-Based Polymer for High-Performance Field-Effect Transistors. Advanced Materials. 2016;28(20):3922-27.
[14] Xu YX, Chueh CC, Yip HL, Chang CY, Liang PW, Intemann J J, Chen WC, Jen AK. Indacenodithieno[3,2-b]thiophene-based broad bandgap polymers for high efficiency polymer solar cells. Polymer Chemistry. 2013; 4(20), 5220-23.
[15] Chang HH, Tsai CE, Lai YY, Chiou DY, Hsu SL, Hsu CS, Cheng YJ. Synthesis, Molecular and Photovoltaic Properties of Donor-Acceptor Conjugated Polymers Incorporating a New Heptacylic Indacenodithieno[3,2-b]thiophene Arene. Macromolecules. 2012; 45(23), 9282-91.
[16] Wu H, Zhao B, Wang W, Guo Z, Wei W, An Z, Gao C, Chen H, Xiao B, Xie Y, Wu H, Cao Y. Side chain modification: an effective approach to modulate the energy level of benzodithiophene based polymers for high-performance solar cells. Journal of Materials Chemistry A. 2015;3(35): 18115-26.
[17] Chen L, Shen P, Zhang ZG, Li Y. Side-chain engineering of benzodithiophene–thiophene copolymers with conjugated side chains containing the electron-withdrawing ethylrhodanine group. Journal of Materials Chemistry A. 2015;3(22): 12005-15.
[18] Jiang JM, Lin HK, Lin YC, Chen HC, Lan SC, Chang CK, Wei KH. Side Chain Structure Affects the Photovoltaic Performance of Two-Dimensional Conjugated Polymers. Macromolecules. 2014;47(1): 70-78.
[19] Li G, Lu Z, Li C, Bo Z. The side chain effect on difluoro-substituted dibenzo[a,c]phenazine based conjugated polymers as donor materials for high efficiency polymer solar cells. Polymer Chemistry. 2015;6(9):1613-1618.
[20] Li G, Zhao B, Kang C, Lu Z, Li C, Dong H, Hu W, Wu H, Bo Z. Side Chain Influence on the Morphology and Photovoltaic Performance of 5-Fluoro-6-alkyloxybenzothiadiazole and Benzodithiophene Based Conjugated Polymers. ACS Applied Materials & Interfaces.2015;7(20):10710-17.
[21] Lee W, Lee C, Yu H, Kim DJ, Wang C, Woo HY, Oh JH, Kim BJ. Side Chain Optimization of Naphthalenediimide–Bithiophene-Based Polymers to Enhance the Electron Mobility and the Performance in All-Polymer Solar Cells. Advanced Functional Materials. 2016;26(10):1543-1553.
[22] Xu X, Li Z, Backe O, Bini K, James DI, Olsson E, Andersson MR, Wang E. Effects of side chain isomerism on the physical and photovoltaic properties of indacenodithieno[3,2-b]thiophene–quinoxaline copolymers: toward a side chain design for enhanced photovoltaic performance. Journal of Materials Chemistry A. 2014;2(44):18988-18997.

[23] Dang D, Chen W, Himmelberger S, Tao Q, Lundin A, Yang R, Zhu W, Salleo A, Müller C, Wang E. Enhanced Photovoltaic Performance of Indacenodithiophene-Quinoxaline Copolymers by Side-Chain Modulation. Advanced Energy Materials. 2014;4(15):1400680.
[24] LinY, Zhao F, He Q, Huo L, Wu Y, Parker TC, Ma W, Sun Y, Wang C, Zhu D, Heeger AJ, Marder SR, Zhan X. High-Performance Electron Acceptor with Thienyl Side Chains for Organic Photovoltaics. Journal of the American Chemical Society. 2016;138 (14): 4955-61.
[25] Yang Y, Zhang ZG, Bin H, Chen S, Gao L, Xue L, Yang C, Li Y. Side-Chain Isomerization on an n-type Organic Semiconductor ITIC Acceptor Makes 11.77% High Efficiency Polymer Solar Cells. Journal of the American Chemical Society. 2016;138 (45):15011-18.
[26] (a) Shi C, Yao Y, Yang Y, Pei Q. Regioregular Copolymers of 3-Alkoxythiophene and Their Photovoltaic Application. Journal of the American Chemical Society. 2006;128 (27):8980-86. (b) Zhang M, Guo X, Ma W, Zhang S, Huo L, Ade H, Hou J. An Easy and Effective Method to Modulate Molecular Energy Level of the Polymer Based on Benzodithiophene for the Application in Polymer Solar Cells. Advanced Materials. 2014;26(13):2089-95.
[27] Xu X, Cai P, Lu Y, Choon NS, Chen J, Ong BS, Hu X. Synthesis of a Novel Low-Bandgap Polymer Based on a Ladder-Type Heptacyclic Arene Consisting of Outer Thieno[3,2-b]thiophene Units for Efficient Photovoltaic Application. Macromolecular Rapid Communications. 2013;34(8): 681-688.
[28] (a) Liao SH, Jhuo HJ, Cheng YS, Chen SA. Fullerene Derivative-Doped Zinc Oxide Nanofilm as the Cathode of Inverted Polymer Solar Cells with Low-Bandgap Polymer (PTB7-Th) for High Performance. Advanced Materials. 2013;25(34):4766-4771. (b) Wang M, Hu X, Liu P, Li W, Gong X, Huang F, Cao Y. Donor–Acceptor Conjugated Polymer Based on Naphtho[1,2-c:5,6-c]bis[1,2,5]thiadiazole for High-Performance Polymer Solar Cells. Journal of the American Chemical Society. 2011;133 (25):9638–41.
[29] He Y, Chen HY, Hou J, Li Y. Indene−C60 Bisadduct: A New Acceptor for High-Performance Polymer Solar Cells. Journal of the American Chemical Society. 2010;132 (4):1377–1382.
[30] Lu L, Zheng T, Xu T, Zhao D, Yu L. Mechanistic Studies of Effect of Dispersity on the Photovoltaic Performance of PTB7 Polymer Solar Cells. Chemistry of Materials. 2015;27(2):537-543.
[31] Qian D, Ye L, Zhang M, Liang Y, Li L, Huang Y, Guo X, Zhang S, Tan Z, Hou J. Design, Application, and Morphology Study of a New Photovoltaic Polymer with Strong Aggregation in Solution State. Macromolecules. 2012:45(24), 9611-17.
[32] Wu Y, Li Z, Ma W, Huang Y, Huo L, Guo X, Zhang M, Ade H, Hou J. PDT-S-T: A New Polymer with Optimized Molecular Conformation for Controlled Aggregation and π–π Stacking and Its Application in Efficient Photovoltaic Devices. Advanced Materials. 2013;25(25): 3449-55.
[33] Li W, Yan L, Zhou H, You W. A General Approach toward Electron Deficient Triazole Units to Construct Conjugated Polymers for Solar Cells. Chemistry of Materials. 2015;27(18): 6470-6476.
[34] Zhou H, Yang L, Stoneking S, You W. A Weak Donor-Strong Acceptor Strategy to Design Ideal Polymers for Organic Solar Cells. ACS Applied Materials & Interfaces. 2010;2(5):1377-1383.
[35] Liu D, Zhao W, Zhang S, Ye L, Zheng Z, Cui Y, Chen Y, Hou J. Highly Efficient Photovoltaic Polymers Based on Benzodithiophene and Quinoxaline with Deeper HOMO Levels. Macromolecules. 2015;48(15): 5172-78.

[36] Wang N, Chen W, Shen W, Duan L, Qiu M, Wang J, Yang C, Du Z, Yang R. Novel donor–acceptor polymers containing o-fluoro-p-alkoxyphenyl-substituted benzo[1,2-b:4,5-b′]dithiophene units for polymer solar cells with power conversion efficiency exceeding 9%. Journal of Materials Chemistry A. 2016;4(26): 10212-10222.
[37] (a) Zhang M, Guo X, Zhang S, Hou J. Synergistic Effect of Fluorination on Molecular Energy Level Modulation in Highly Efficient Photovoltaic Polymers. Advanced Materials. 2014;26(7):1118-23. (b) Genene Z, Wang J, Xu X, Yang R, Mammo W, Wang E. A comparative study of the photovoltaic performances of terpolymers and ternary systems. RSC Advances. 2017,**7**:17959-17967
[38] Lu Y, Xiao Z, Yuan Y, Wu H, An Z, Hou Y, Gao C, Huang J. Fluorine substituted thiophene–quinoxaline copolymer to reduce the HOMO level and increase the dielectric constant for high open-circuit voltage organic solar cells. Journal of Materials Chemistry C. 2013;1(4):630-637.
[39] (a) Chen HC, Chen YH, Liu CC, Chien YC, Chou SW, Chou PT. Prominent Short-Circuit Currents of Fluorinated Quinoxaline-Based Copolymer Solar Cells with a Power Conversion Efficiency of 8.0%. Chemistry of Materials. 2012;24(24):4766-4772. (b) Cong Z, Zhao B, Wu H, Guo Z, Wang W, Luo G, Xu J, Xia Y, Gao C, An Z. Synthesis of copolymers based on benzo[1,2-b:4,5-b′]difuran and fluorinated quinoxaline derivatives and their photovoltaic properties. Polymer. 2015; 67: 55-62. (c) Wang E, Hou L, Wang Z, Hellström S, Zhang F, Inganäs O, Andersson MR. An easy synthesized blue polymer for high-performance polymer solar cells. Avanced Materials. 2010; 22(46):5240-5244. (d) Wang E, Bergqvist J, Vandewal K, Ma Z, Hou L, Lundin A, Himmelberger S, Salleo S, Müller C, Inganäs O, Zhang F, Andersson MR. Conformational disorder enhances solubility and photovoltaic performance of a thiophene–quinoxaline copolymer. Advanced Energy Materials. 2013; 3(6): 806-814.
[40] (a) Zhou C, Zhang G, Zhong C, Jia X, Luo P, Xu R, Gao K, Jiang X, Liu F, Russell TP, Huang F, Cao Y. Toward High Efficiency Polymer Solar Cells: Influence of Local Chemical Environment and Morphology Advanced Energy Materials. 2017;7(1): 1601081. (b) Zhong W, Liang J, Hu S, Jiang XF, Ying L, Huang F, Yang W, Cao Y. Effect of Monofluoro Substitution on the Optoelectronic Properties of Benzo[c][1,2,5] thiadiazole Based Organic Semiconductors. Macromolecules. 2016;49(16):5806-16.
[41] (a) Cong Z, Liu S, Zhao B, Wang W, Liu H, Su J, Guo Z, Wei W, Gao C, An Z. High performance alternating polymers based on two-dimensional conjugated benzo[1,2-b:4,5-b′]dithiophene and fluorinated dithienylbenzothiadiazole for solar cells. RSC Advances. 2016; 6:77525-34. (b) Dutt GK, Kim T, Choi H, Lee J, Kim DS, Kim JY, Yang C. Synthesis of fluorinated analogues of a practical polymer TQ for improved open-circuit voltages in polymer solar cells. Polymer Chemistry. 2014;5(7):2540-2547.
[42] Pommerehne J, Vestweber H, Guss W, Mahrt RF, Bässler H, Porsch M, Daub J. Efficient two layer leds on a polymer blend basis. Advanced Materials. 1995;7(6):551-54.
[43] Hou J, Tan Z, Yan Y, He Y, Yang C, Li Y. Synthesis and Photovoltaic Properties of Two-Dimensional Conjugated Polythiophenes with Bi(thienylenevinylene) Side Chains. Journal of the American Chemical Society. 2006;128 (14):4911–16.
[44] (a) Kroon R, Gehlhaar R, Steckler TT, Henriksson P, Muller C, Bergqvist J, Hadipour A, Heremans P, Andersson MR. New quinoxaline and pyridopyrazine-based polymers for solution-processable photovoltaics. Solar Energy Materials and Solar Cells. 2012;105: 280-286.(b) Dutt GK, Kim T, Choi H, Lee J, Kim DS, Kim JY, Yang C. Synthesis of fluorinated analogues of a

practical polymer TQ for improved open-circuit voltages in polymer solar cells. Polymer Chemistry. 2014;5(7):2540-2547.
[45] He ZC, Zhong CM, Huang X, Wong WY, Wu HB, Chen LW, Su SJ, Cao Y. Simultaneous Enhancement of Open-Circuit Voltage, Short-Circuit Current Density, and Fill Factor in Polymer Solar Cells. Advanced Materials. 2011;23(40):4636-43.
[46] Liu X, Wang H, Yang T, Zhang W, Gong X. Solution-Processed Ultrasensitive Polymer Photodetectors with High External Quantum Efficiency and Detectivity. ACS Applied Materials & Interfaces. 2012; 4(7):3701-3705.
[47] Miao J, Chen H, Liu F, Zhao B, Hu L, He Z, Wu H. Efficiency enhancement in solution-processed organic small molecule: Fullerene solar cells via solvent vapor annealing. Applied Physics Letters. 2015;106:183302.
[48] Zhao B, Wu H, Liu S, Luo G, Wang W, Guo Z, Wei W, Gao C, An Z. Efficient alternating polymer based on benzodithiophene and di-fluorinated quinoxaline derivatives for bulk heterojunction photovoltaic cells. Polymer. 2017;116:35-42.
[49] Liu C, Wang K, Hu X, Yang Y, Hsu C-H, Zhang W, Xiao S, Gong X, Cao Y. Molecular Weight Effect on the Efficiency of Polymer Solar Cells. ACS Applied Materials & Interfaces. 2013;5(22):12163−12167
[50] Son HJ, Wang W, Xu T, Liang Y, Wu Y, Li G, Yu L. Synthesis of Fluorinated Polythienothiophene-co-benzodithiophenes and Effect of Fluorination on the Photovoltaic Properties. Journal of the American Chemical Society. 2011;133(6):1885-94.

Highlights

1. Six alternating polymers based on alkoxy-phenyl substituted IDT and quinoxaline derivatives were synthesized.

2. All polymers showed high molecular weight, finely tunable bandgaps and gradient adjusted energy levels.

3. A PCE of 5.97% was achieved for the fluorinated IDT-based polymer **FO-TQ** blended with $PC_{71}BM$.